



## A selective intra-HN(CA)CO experiment for the backbone assignment of deuterated proteins

Daniel Nietlispach

Contribution from the Cambridge Centre for Molecular Recognition, Department of Biochemistry, University of Cambridge, 80 Tennis Court Road, Cambridge, CB2 1GA, U.K. (E-mail: dn0@bioc.cam.ac.uk)

Received 17 June 2003; Accepted 22 August 2003

**Key words:** backbone resonance assignment, deuteration, TROSY

### Abstract

A modified version of the backbone TROSY based 3D HN(CA)CO experiment is presented that provides uniquely intraresidue correlation shift information, by efficiently suppressing the sequential connectivity data. The resulting reduction in the number of peaks decreases overlap and removes ambiguities in situations where in the conventional HN(CA)CO  $i$  and  $i - 1$  correlations are overlapped or are comparable in intensity. The sequential residue connection is obtained in combination with a 3D HNCO. MQ- and SQ-implementations of the experiment were tested on a deuterated protein with a correlation time of 28 ns ( $\sim 60$  kDa).

### Introduction

The backbone assignment is one of the first steps in an NMR protein structure determination. Triple-resonance experiments recorded on  $^{13}\text{C}$ ,  $^{15}\text{N}$  labelled proteins allow this to be achieved in an efficient manner, nowadays allowing proteins up to a size of 20 kDa to be routinely assigned (Sattler et al., 1999). Over the last few years, a range of triple-resonance TROSY based experiments have been introduced that allow the sequential residue assignment of larger  $^2\text{H}$ ,  $^{13}\text{C}$ ,  $^{15}\text{N}$  labelled proteins (Pervushin et al., 1997; Salzmann et al., 1999a, b; Yang and Kay, 1999b). Several of these strategies rely on a constant-time (Santoro and King, 1992; Vuister and Bax, 1992) approach to provide the necessary resolution in the  $^{13}\text{C}$  dimension and focus on HNCA/HN(CO)CA based experiments (Ikura et al., 1990; Grzesiek and Bax, 1992; Yamazaki et al., 1994a, b), and if sensitivity permits HNCACB/HN(CO)CACB experiments (Witek and Mueller, 1993; Yamazaki et al., 1994a), to achieve the sequential correlation.

Ambiguities in the HNCA/HN(CO)CA based sequential assignment approach that result from  $^{13}\text{C}^\alpha$  shift degeneracy can often be resolved using the HN(CA)CO/HNCO 3D experiments (Kay et al., 1990;

Clubb et al., 1992; Grzesiek and Bax, 1992; Matsuo et al., 1996), which provide the sequential connectivity through matching of the  $^{13}\text{C}'$  chemical shifts. Such experiments benefit from the fact that  $^{13}\text{C}'$  chemical shifts correlate less with the residue type (Sayers and Torchia, 2001) and can be particularly useful in situations where the sensitivity of the  $^{13}\text{C}^\beta$  directed experiments is insufficient. Several groups have reported backbone assignments using 3D TROSY experiments of slowly tumbling proteins where the number of residues are limited, for example in homooligomers and detergent-solubilised membrane proteins (Salzmann et al., 2000; Arora et al., 2001; Fernandez et al., 2001a, b). In these cases the resolution attainable by 3D NMR is sufficient for assignment. A more recent approach used the advantageous spectral resolution of 4D NMR spectroscopy to assign the resonances of a 723 residue protein (Yang and Kay, 1999a; Tugarinov et al., 2002).

HNCA and HNCACO out-and-back experiments provide correlations to both the same and the preceding residue. The presence of two peaks per  $^1\text{HN}/^{15}\text{N}$  pair can unnecessarily complicate these spectra and lead to potential ambiguities in the assignment of larger proteins due to increased overlap. To alleviate this situation we, and others recently introduced a new

intra-HNCA experiment (Brutscher, 2002; Nietlispach et al., 2002; Permi, 2002) that selects specifically for the intraresidue correlation, resulting in one peak per  $^1\text{HN}/^{15}\text{N}$  spin pair. In a further development of this work it is shown in this contribution that a similar approach can be applied to the HN(CA)CO experiment, resulting in a selective intra-HN(CA)CO pulse sequence, correlating  $^1\text{HN}_i$ ,  $^{15}\text{N}_i$  and  $^{13}\text{C}'_i$  nuclei in a 3D experiment. The sequential connectivity can be obtained with the complementary 3D HNCO.

## Materials and methods

A sample of 0.9 mM  $^{15}\text{N}$ ,  $^{13}\text{C}$ ,  $^2\text{H}$  [Ile( $\delta_1$  only), Leu, Val]-methyl-protonated H-Ras (1–171)-GDP in 20 mM phosphate buffer (pH 6.5), 35 mM sodium chloride, 5 mM magnesium chloride, 10 mM DTT, 0.01%  $\text{NaN}_3$  and 7%  $\text{D}_2\text{O}$  was used. The experiments were recorded on a Bruker Avance 600 MHz spectrometer equipped with a 5 mm TXI HCN/z probe. All data sets were recorded at 4°C with (16, 36, 512) complex points in ( $t_1$ ,  $t_2$ ,  $t_3$ ) corresponding to acquisition times of (8, 18, 51 ms). 16 scans per FID (1.6 s relaxation delay) were recorded resulting in a total experiment time of 21 h. The data was processed in AZARA (Wayne Boucher, unpublished) and analysed using ANSIG (Kraulis, 1989). For comparative purposes conventional HN(CA)CO experiments were recorded, modified according to the legend of Figure 1.

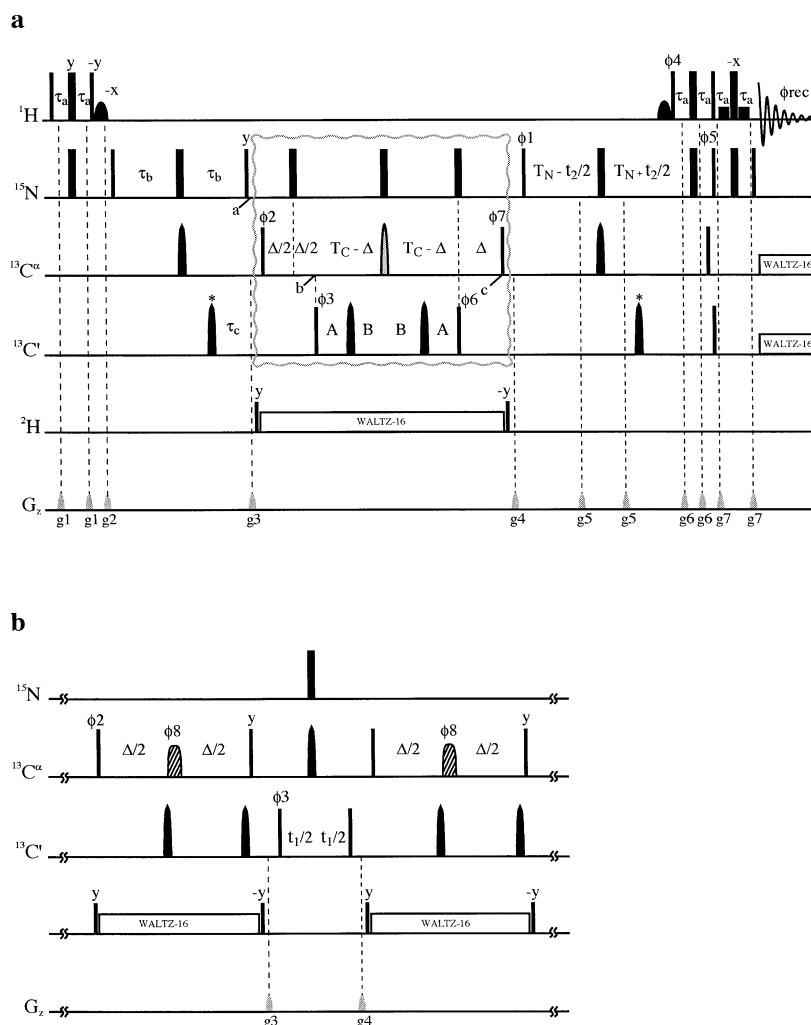
## Results and discussion

Figure 1 shows the TROSY intra-HN(CA)CO pulse sequence that selects for the intraresidue transfer pathway. In what follows a brief outline of the essential transfer steps of this out-and-back experiment are described and the basic principles leading to the intra-selectivity are given. Initial proton coherence is transferred to  $^{15}\text{N}$ , which evolves under both  $^{1,2}J_{\text{N,Ca}}$  coupling constants simultaneously, into terms antiphase with respect to  $^{13}\text{C}^\alpha$ . Typically this transfer is normally optimized either for  $^1J$  or  $^2J$ , whereas here the length of the transfer period  $2\tau_b$  is increased such as to maximize the buildup of the doubly antiphase term  $\text{N}_x\text{C}^\alpha(i)_z\text{C}^\alpha(i-1)_z$ , as described previously (Nietlispach et al., 2002). At the same time, the evolution due to  $^1J_{\text{N,C}'}$  is enabled so that at point **a** (Figure 1a) in the sequence magnetization of the form

$8\text{N}_x\text{C}^\alpha(i)_z\text{C}^\alpha(i-1)_z\text{C}'_z$  is generated, whereas the remaining  $^{13}\text{C}^\alpha$  singly antiphase operators are destroyed by the action of the pulsed field gradient  $g_3$ . The buildup efficiency of the doubly antiphase term, the effects of  $^{15}\text{N}$  relaxation and variations in the size of  $^{1,2}J_{\text{N,Ca}}$  are described in detail elsewhere (Nietlispach et al., 2002) and shall only be outlined here. In brief, in the absence of relaxation, doubly antiphase coherence can be created in larger amounts than singly antiphase terms, to an extent that, even in the presence of  $^{15}\text{N}$  transverse relaxation and with the longer transfer time  $2\tau_b$  required, the generation of the doubly antiphase term remains competitive.

From point **a** in the sequence, the first  $^{13}\text{C}$   $90^\circ$  pulse creates  $^{13}\text{C}^\alpha$  multiple-quantum coherence, which subsequently evolves during the period  $\Delta$  under the two  $^1J_{\text{Ca,C}'}$  couplings to the directly attached carbonyl spins, resulting in the complete refocusing of the  $^{13}\text{C}'$  operator contribution from the  $i-1$  residue at point **b**, whilst simultaneously transferring through the intraresidue  $^1J_{\text{Ca,C}'}$  coupling. As this transfer step removes the  $i-1$   $^{13}\text{C}'$  operator dependence and introduces at the same time the  $^{13}\text{C}'_i$  spin term, it provides the basic mechanism for the intraresidue selectivity of the pulse sequence. After the first  $^{13}\text{C}'$   $90^\circ$  pulse, the  $^{13}\text{C}'_i$  chemical shift is recorded in a CT manner, followed by the reverse evolution of both  $^1J_{\text{Ca,C}'}$  couplings to restore the  $^{13}\text{C}^\alpha$ -MQ-term antiphase with respect to the  $^{13}\text{C}'$  of the preceding residue at point **c**. Finally, back-transfer to  $^{15}\text{N}$ , chemical shift labelling and refocusing under  $^{1,2}J_{\text{Ca,N}}$  and  $^1J_{\text{Ca,C}'}$  is completed by a phase-cycled sensitivity enhanced TROSY module. Here any type of TROSY scheme can be used, including the shorter, concatenated version where  $J_{\text{N,Ca}}$  and  $J_{\text{N,C}'}$  refocusing also proceeds during the period  $2\tau_a$  (Salzmann et al., 1999c). The longer  $^{15}\text{N}$  transfer period  $2T_{\text{N}}$  allows for higher resolution in the  $^{15}\text{N}$  dimension. The longer transfer time benefits greatly from slower  $^{15}\text{N}$  relaxation, making the TROSY implementation for slower tumbling proteins more attractive ( $\tau_m > 15$  ns).

The HMQC-style implementation of the  $^{13}\text{C}^\alpha/^{13}\text{C}'$  coherence transfer of Figure 1a (abbreviated as MQ-CACO) allows the  $^{13}\text{C}^\alpha$  transverse period  $2T_{\text{C}}$  to be set to a value  $1/J_{\text{Ca,Cb}}$  in order to refocus the effects from the passive couplings to both  $^{13}\text{C}^\beta$  nuclei. This reduces sensitivity losses that would occur from partial  $J_{\text{Ca,Cb}}$  dephasing, without the need to resort to selective  $^{13}\text{C}^\alpha$  pulses or selective adiabatic  $^{13}\text{C}^\beta$  decoupling. Similar implementations of a CT-HMQC-based  $^{13}\text{C}^\alpha/^{13}\text{C}'$  transfer have been suggested before



**Figure 1.** Pulse scheme of the 3D intra-HN(CA)CO with a MQ- $^{13}\text{C}^\alpha/^{13}\text{C}'$  transfer scheme (a). The boxed region in Figure 1a can be replaced by the scheme of Figure 1b, resulting in the SQ- $^{13}\text{C}^\alpha/^{13}\text{C}'$  version of the experiment (b). All narrow and wide black vertical lines are applied as rectangular  $90^\circ$  and  $180^\circ$  pulses, respectively, along the  $x$ -axis unless indicated differently. The carriers for  $^1\text{H}$ ,  $^2\text{H}$ ,  $^{13}\text{C}$ ,  $^{13}\text{C}'$  and  $^{15}\text{N}$  are set at the frequency of 4.75 ppm, 4.0 ppm, 56.0 ppm, 176.0 ppm and 119.4 ppm, respectively. For the MQ-version separate frequency control units are used for  $^{13}\text{C}$  ( $^{13}\text{C}^\alpha$ ,  $^{13}\text{C}^\beta$ ) and  $^{13}\text{C}'$  nuclei. All  $^1\text{H}$  pulses are applied with a 23 kHz field, except the shaped E-SNOB (Kupce et al., 1995) (2.1 ms, 0.27 kHz) and the low-power square  $90^\circ$  pulses (1.4 ms).  $^{15}\text{N}$  pulses employ a 6.1 kHz field, and  $^2\text{H}$   $90^\circ$  square pulses and the WALTZ-16 decoupling sequence are applied with a 0.8 kHz field. All rectangular  $90^\circ$  pulses applied to  $^{13}\text{C}^\alpha$  and  $^{13}\text{C}'$  have a length of 53.5  $\mu\text{s}$  (at 600 MHz) so as to minimize excitation at the corresponding  $^{13}\text{C}'$  or  $^{13}\text{C}^\alpha$  frequencies, respectively. All shaped  $180^\circ$   $^{13}\text{C}'$  pulses and the  $^{13}\text{C}^\alpha$  inversion pulses during the  $^{15}\text{N}$  transfer periods are applied with a G3 profile (Emsley and Bodenhausen, 1990) of 512  $\mu\text{s}$  duration (7.01 kHz peak power). The  $180^\circ$   $^{13}\text{C}^\alpha$  pulse (grey shaded) in the centre of  $2T_C$  is applied as 256  $\mu\text{s}$  REBURP pulse (Geen and Freeman, 1991) (24.4 kHz peak field strength). The pulses with phase  $\phi_8$  have a length of 1.6 ms (REBURP, 3.9 kHz, applied at 56.0 ppm) in order to selectively refocus  $^{13}\text{C}^\alpha$  spins while not inverting  $^{13}\text{C}^\beta$ . A 120  $\mu\text{s}$  sinc shaped profile ( $180^\circ$ , 7.08 kHz) is used as inversion pulse in the centre of the  $t_1$  period. Care is taken to maximize the sensitivity by adjusting the pulse phases  $\phi_6$ ,  $\phi_7$  and  $\phi_8$ , respectively. If required  $^{13}\text{C}^\alpha$  and  $^{13}\text{C}'$  decoupling during the acquisition time can be achieved using a 60 ppm cosine-modulated WALTZ-16 (Shaka et al., 1983) field, centred at 116 ppm, employing pulses that have the SEDUCE-1 profile (McCoy and Mueller, 1992) (300  $\mu\text{s}$   $90^\circ$  pulses, 3.6 kHz peak power). The delays used are  $\tau_a = 2.25$  ms,  $\tau_b = 24.0$  ms,  $\tau_c = 16$  ms,  $\Delta = 4.5$  ms,  $T_C = 14.0$  ms,  $T_N = 24.0$  ms,  $A = (2T_C - 2\Delta + t_1)/4$ ,  $B = (2T_C - 2\Delta - t_1)/4$ . The phase cycle is  $\phi_1 = (y, -y, -x, x)$ ,  $\phi_2 = 4(x), 4(-x)$ ,  $\phi_3 = 8(x), 8(-x)$ ,  $\phi_4 = y$ ,  $\phi_5 = y$ ,  $\phi_6 = x - 56^\circ$ ,  $\phi_7 = x - 5^\circ$ ,  $\phi_8 = x - 3^\circ$ ,  $\phi_{\text{rec}} = 2(y, -y, -x, x), 2(-y, y, x, -x)$ . Quadrature detection in the  $F_2$  dimension ( $^{13}\text{C}'$ ) is achieved using States-TPPI (Marion et al., 1989) of  $\phi_3$  while in the  $F_1$  dimension ( $^{15}\text{N}$ ) a phase-sensitive spectrum is obtained by recording a second FID for each increment of  $t_2$ , with  $\phi_1 = (y, -y, x, -x)$  and the phases of  $\phi_4$  and  $\phi_5$  inverted. For each successive  $t_2$  increment,  $\phi_1$  and the phase of the receiver are incremented by  $180^\circ$ , and the data are processed as described by Kay et al. (1992). The duration and strengths of the sine-bell shaped gradients are  $g_1 = (0.4$  ms, 5 G/cm),  $g_2 = (1.1$  ms, 11 G/cm),  $g_3 = (1.3$  ms, 15 G/cm),  $g_4 = (0.9$  ms, 11 G/cm),  $g_5 = (0.5$  ms, 11 G/cm),  $g_6 = (0.9$  ms, 17 G/cm),  $g_7 = (0.6$  ms, 21 G/cm). Conventional, non-selective versions of both experiments can be obtained with  $\tau_b = 12$  ms, omitting the  $^{13}\text{C}'$   $180^\circ$  pulses marked with an asterisk and by letting the receiver phase follow  $\phi_2$ .

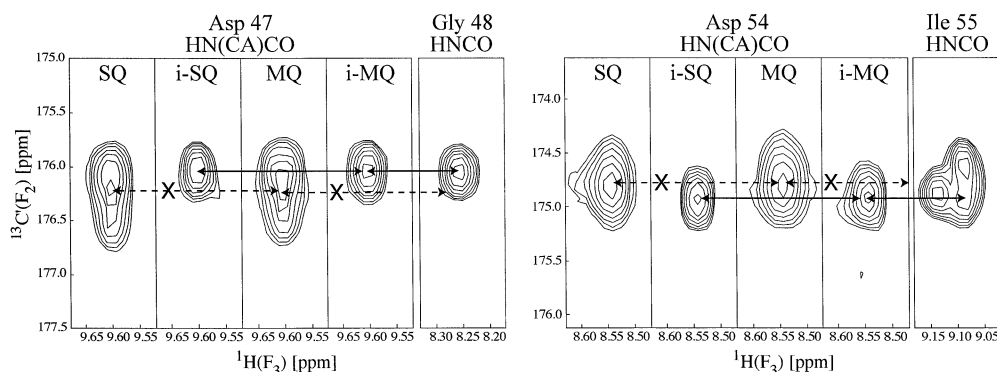


Figure 2. Selected strip plots from the 3D intra-HN(CO)CA (i-MQ and i-SQ) and the corresponding non-selective experiments (MQ and SQ) for the residues Asp 47 and Asp 54, illustrating the benefits of the reduced number of peaks in the selective experiments. SQ and MQ refer to the single- or multiple-quantum  $^{13}\text{C}^\alpha/^{13}\text{C}'$  transfer schemes, respectively, according to Figure 1. In both cases the reduced ambiguity in the  $^{13}\text{C}'$  dimension of the intra-experiments allows the successful match with the  $i + 1$  HNCOC resonance of residues 48 and 55, whilst using the conventional HN(CA)CO, overlap of the  $i$  and  $i - 1$  resonances complicates the sequential assignment.

(Bazzo et al., 1995; Engelke and Rueterjans, 1995; Loria et al., 1999), with the difference being that in the intra experiment two  $^{13}\text{C}^\alpha$  spins are transverse. The CT approach can offer enhanced sensitivity for the observation of Ser residues, where  $^{13}\text{C}^\alpha$  and  $^{13}\text{C}^\beta$  shifts tend to be close together, or residues Gly, Val and others where  $^{13}\text{C}^\alpha$  shifts may be outside the bandwidth of a chosen  $^{13}\text{C}^\alpha$  selective refocusing pulse. Equally, since the term of interest evolves in the form of  $^{13}\text{C}_i^\alpha/^{13}\text{C}_{i-1}^\alpha$  multiple-quantum coherence, the same benefits also apply to residues that are preceded by one of the aforementioned amino acids. The length of the  $^{13}\text{C}'$  evolution period is limited to a CT of approximately 9–10 ms but can be doubled by mirror image linear prediction. Alternatively, the period in Figure 1a between the pulses with phase  $\phi_2$  and  $\phi_7$  can be replaced by a shorter HSQC-type  $^{13}\text{C}^\alpha/^{13}\text{C}'$  transfer scheme (SQ-CACO) as shown by the insert of Figure 1b. This essentially follows the implementation previously described by Kay and co-workers (Yang and Kay, 1999a; Tugarinov et al., 2002).

Both 3D TROSY experiments of Figure 1 were tested on a 0.9 mM sample of  $^2\text{H}$ ,  $^{13}\text{C}$ ,  $^{15}\text{N}$  labelled H-Ras (1–171)-GDP at 4 °C. Under these conditions the correlation time of the protein is approximately 28 ns corresponding to a protein of approximately 60 kDa. Conventional non-selective HN(CA)CO versions of the two experiments were also performed using  $2\tau_b$  and  $2T_N$  periods of 24 ms, and omitting the  $^{13}\text{C}'$   $180^\circ$  pulses marked by an asterisk (Figure 1). Representative strip plots of the MQ- and SQ-CACO versions of the TROSY intra-HN(CA)CO for Asp 47 and Asp 54 are shown in Figure 2 together with the corresponding

planes of the non-selective HN(CA)CO TROSY experiments and the HNCOC plots at the  $i + 1$  position. Both cases are characteristic of the situation where overlap of the  $i$  and  $i - 1$  peaks in the non-selective experiments precludes progression of the sequential assignment. In contrast, with the information from the intra-HN(CA)CO experiments, the  $^{13}\text{C}'$  chemical shift match with the HNCOC resonance can be done in an unambiguous manner, allowing the assignment to proceed via the sequential  $i$  to  $i + 1$  connection. The plots from both selective versions of the experiments (i-MQ, i-SQ) contain solely the intraresidue correlation. This shows that the values of the  $^1J_{\text{Ca},\text{C}'}$  couplings are sufficiently uniform to allow efficient suppression of the sequential pathway as described above. For all of the 154 observed correlations, the inter-residue contribution is successfully suppressed.

Figure 3a shows examples where in SQ-CACO versions of the experiments the use of selective  $^{13}\text{C}^\alpha$  pulses reduces the peak intensities, whereas in both MQ-CACO style experiments (selective and non-selective) the  $i$  resonance is present and again, unambiguous information is provided in the intra-experiment. While all 8 Ser residues of Ras are observed in the i-MQ and MQ versions, 6 are missing in the SQ-versions of the experiment. Strip plots of Val 152 demonstrate (Figure 3a), that residues with  $^{13}\text{C}^\alpha$  shifts  $> 63$  ppm are attenuated in the SQ-CACO type experiments as a consequence of the limited  $^{13}\text{C}^\alpha$  refocusing bandwidth.

Further information can be derived from the phase properties of the observed signals. The SQ-CACO versions are not sensitive to the type of residue. In the

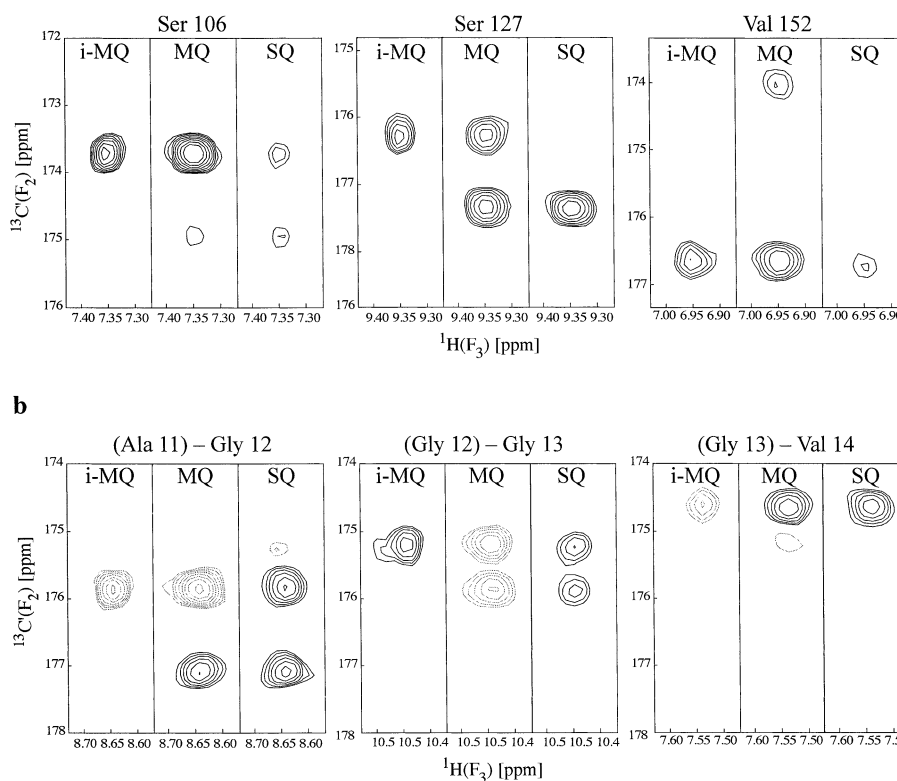


**Figure 3.** (a) Effects of the  $^{13}\text{C}^\alpha$ -selective  $180^\circ$  pulses in the SQ experiments: Residues with similar  $^{13}\text{C}^\alpha$  and  $^{13}\text{C}^\beta$  shifts (e.g., Ser 106 and Ser 127) or residues with  $^{13}\text{C}^\alpha$  outside the refocusing bandwidth (e.g., Val 152) are strongly attenuated in the SQ implementations but are observable in both constant time MQ experiments (i-SQ planes are not shown due to lack of signal). (b) Influence of  $^1J_{\text{Ca,C}\beta}$  evolution on the sign of peaks. The CT- $^{13}\text{C}^\alpha$  period inverts the peaks of Gly in both MQ experiments. Moreover, in the i-MQ experiment residues preceded by a Gly are also inverted, while two sequential Gly result in a positive signal (negative contours are shown in grey). The peaks in the SQ versions are insensitive to the type of residue.

non-selective MQ experiment, each Gly peak appears with the opposite sign, while in the case of the MQ-CACO intra-HN(CA)CO the final sign of an observed signal depends on the  $^{13}\text{C}^\alpha$  properties of both residues  $i$  and  $i - 1$ , leading to positive  $i$  signals if both or none of the two residues are Gly, or negative signals if only one of the two residues is a Gly, as shown in Figure 3b. Therefore the intra-MQ experiment allows the recognition of Gly – X, Gly – Gly and X – Gly pairs (X = non-Gly residue) uniquely from the shift and sign information of the  $i$  resonance.

The comparison of the Ras spectra recorded at  $4^\circ\text{C}$  (correlation time of 28 ns) reveals that the sensitivity of the two versions of the intra-HN(CA)CO experiment is on average 20–30% lower than for the corresponding conventional TROSY HN(CA)CO. Clearly, the presence of  $^{13}\text{C}^\alpha$  multiple-quantum coherence over extended periods of time reduces the overall sensitivity of the intra experiments due to fast trans-

verse relaxation. Even with high levels of deuteration  $^{13}\text{C}^\alpha$  transverse relaxation can be substantial in larger proteins, so that the use of shorter  $^{13}\text{C}^\alpha$  transverse periods is desirable. Under such conditions the i-SQ-CACO type implementation can be of advantage as the duration of the  $^{13}\text{C}^\alpha$  transverse period is reduced by 35%, to approximately  $1/J_{\text{Ca,C}\beta}$ . For Ser, for residues with a  $^{13}\text{C}^\alpha$  chemical shift  $> 63$  ppm or those following such residues, this advantage is unfortunately often offset by the abovementioned bandwidth effects of the selective  $^{13}\text{C}^\alpha$  pulses, making the outcome less predictable, particularly if  $^{13}\text{C}^\alpha$  chemical shifts are *a priori* not known. Despite the reduced sensitivity, and with the exception of 3 residues, all intraresidue correlations that have a matching HNCO peak are observed in the i-MQ-CACO implementation. Hence the initial use of the i-MQ version of the selective experiment is preferred over the i-SQ pulse sequence. An additional 7 sequential correlations could be made,

which due to  $i/i - 1$   $^{13}\text{C}'$  shift degeneracy remained ambiguous in the conventional HN(CA)CO/HNCO experiments.

For proteins with a correlation time  $> 20$  ns the sensitivity of the intra experiments is likely to be lower than for the non-selective HN(CA)CO where only one  $^{13}\text{C}'$  spin is transverse at the time. Even so, the benefits from the reduced overlap more than compensate for the decreased sensitivity. An upper limit for the usefulness of the intra experiment is estimated for proteins with a correlation time of 30 ns. For smaller deuterated proteins  $^{13}\text{C}'$  relaxation is less problematic, leading to similar intensities between intra- and non-selective experiments. For a correlation time of 12 ns (for example Ras at 25 °C) intra- versus non-selective experiments show comparable sensitivity when using a  $^1\text{H}/^{15}\text{N}$  INEPT transfer scheme, or higher relative sensitivity with a TROSY scheme. In such cases therefore the obtainable spectral improvements come at no additional loss.

## Conclusions

In summary, a new 3D intra-HN(CA)CO backbone experiment is presented that selectively suppresses the  $i - 1$  correlation, resulting in spectra with reduced overlap and providing unambiguous  $^{13}\text{C}'_i$  shift assignments. This is of particular advantage in situations where  $i$  and  $i - 1$   $^{13}\text{C}'$  shifts are degenerate. The experiment can be used with a MQ- or SQ-CACO transfer scheme and was tested on a deuterated protein with a correlation time of 28 ns.

## Acknowledgements

The Cambridge Centre for Molecular Recognition is supported by the BBSRC and the Wellcome Trust. The author would like to thank Drs Katherine Stott and Helen Mott for reviewing the manuscript and for helpful discussions and Drs Yutaka Ito and Minoru Hatanaka for kindly preparing the H-Ras sample.

## References

Arora, A., Abildgaard, F., Bushweller, J.H. and Tamm, L.K. (2001) *Nat. Struct. Biol.*, **8**, 334–338.  
 Bazzo, R., Cicero, D.O. and Barbato, G. (1995) *J. Magn. Reson. Ser. B*, **107**, 189–191.  
 Brutscher, B. (2002) *J. Magn. Reson.*, **156**, 155–159.

Clubb, R.T., Thanabal, V. and Wagner, G. (1992) *J. Magn. Reson.*, **97**, 213–217.  
 Emsley, L. and Bodenhausen, G. (1990) *Chem. Phys. Lett.*, **165**, 469–476.  
 Engelke, J. and Rueterjans, H. (1995) *J. Magn. Reson. Ser. B*, **109**, 318–322.  
 Fernandez, C., Adeishvili, K. and Wüthrich, K. (2001a) *Proc. Natl. Acad. Sci. USA*, **98**, 2358–2363.  
 Fernandez, C., Hilty, C., Bonjour, S., Adeishvili, K., Pervushin, K. and Wüthrich, K. (2001b) *FEBS Lett.*, **504**, 173–178.  
 Geen, H. and Freeman, R. (1991) *J. Magn. Reson.*, **93**, 93–141.  
 Grzesiek, S. and Bax, A. (1992) *J. Magn. Reson.*, **96**, 432–440.  
 Ikura, M., Kay, L.E. and Bax, A. (1990) *Biochemistry*, **29**, 4659–4667.  
 Kay, L.E., Ikura, M., Tschudin, R. and Bax, A. (1990) *J. Magn. Reson.*, **89**, 496–514.  
 Kay, L.E., Keifer, P. and Saarinen, T. (1992) *J. Am. Chem. Soc.*, **114**, 10663–10665.  
 Kraulis, P.J. (1989) *J. Magn. Reson.*, **84**, 627–633.  
 Kupce, E., Boyd, J. and Campbell, I.D. (1995) *J. Magn. Reson. Ser. B*, **106**, 300–303.  
 Loria, J.P., Rance, M. and Palmer, A.G. (1999) *J. Magn. Reson.*, **141**, 180–184.  
 Marion, D., Ikura, M., Tschudin, R. and Bax, A. (1989) *J. Magn. Reson.*, **85**, 393–399.  
 Matsuo, H., Kupce, E., Li, H.J. and Wagner, G. (1996) *J. Magn. Reson. Ser. B*, **111**, 194–198.  
 McCoy, M.A. and Mueller, L. (1992) *J. Am. Chem. Soc.*, **114**, 2108–2112.  
 Nietlispach, D., Ito, Y. and Laue, E.D. (2002) *J. Am. Chem. Soc.*, **124**, 11199–11207.  
 Permi, P. (2002) *J. Biomol. NMR*, **23**, 201–209.  
 Pervushin, K., Riek, R., Wider, G. and Wüthrich, K. (1997) *Proc. Natl. Acad. Sci. USA*, **94**, 12366–12371.  
 Salzmänn, M., Pervushin, K., Wider, G., Senn, H. and Wüthrich, K. (1999a) *J. Biomol. NMR*, **14**, 85–88.  
 Salzmänn, M., Wider, G., Pervushin, K., Senn, H. and Wüthrich, K. (1999b) *J. Am. Chem. Soc.*, **121**, 844–848.  
 Salzmänn, M., Wider, G., Pervushin, K. and Wüthrich, K. (1999c) *J. Biomol. NMR*, **15**, 181–184.  
 Salzmänn, M., Pervushin, K., Wider, G., Senn, H. and Wüthrich, K. (2000) *J. Am. Chem. Soc.*, **122**, 7543–7548.  
 Santoro, J. and King, G.C. (1992) *J. Magn. Reson.*, **97**, 202–207.  
 Sattler, M., Schleucher, J. and Griesinger, C. (1999) *Prog. Nucl. Magn. Reson. Spectrosc.*, **34**, 93–158.  
 Sayers, E.W. and Torchia, D.A. (2001) *J. Magn. Reson.*, **153**, 246–253.  
 Shaka, A.J., Keeler, J. and Freeman, R. (1983) *J. Magn. Reson.*, **53**, 313–340.  
 Tugarinov, V., Muhandiram, R., Ayed, A. and Kay, L.E. (2002) *J. Am. Chem. Soc.*, **124**, 10025–10035.  
 Vuister, G.W. and Bax, A. (1992) *J. Magn. Reson.*, **98**, 428–435.  
 Wittekind, M. and Mueller, L. (1993) *J. Magn. Reson. Ser. B*, **101**, 201–205.  
 Yamazaki, T., Lee, W., Arrowsmith, C.H., Muhandiram, D.R. and Kay, L.E. (1994a) *J. Am. Chem. Soc.*, **116**, 11655–11666.  
 Yamazaki, T., Lee, W., Revington, M., Mattiello, D.L., Dahlquist, F.W., Arrowsmith, C.H. and Kay, L.E. (1994b) *J. Am. Chem. Soc.*, **116**, 6464–6465.  
 Yang, D.W. and Kay, L.E. (1999a) *J. Am. Chem. Soc.*, **121**, 2571–2575.  
 Yang, D.W. and Kay, L.E. (1999b) *J. Biomol. NMR*, **13**, 3–10.